Virology 510 (2017) 165–174

Contents lists available at ScienceDirect

Virology

journal homepage: www.elsevier.com/locate/yviro

Two-amino acids change in the nsp4 of SARS coronavirus abolishes viral replication

Yusuke Sakai[a,d,1], Kengo Kawachi[a,b,1], Yutaka Terada[a], Hiroko Omori[c], Yoshiharu Matsuura[b], Wataru Kamitani[a,e,*]

[a] Laboratory of Clinical Research on Infectious Diseases, Osaka, Japan
[b] Department of Molecular Virology, Osaka, Japan
[c] Core Instrumentation Facility, Research Institute for Microbial Diseases, Osaka University, Osaka, Japan
[d] Laboratory of Veterinary Pathology, Joint Faculty of Veterinary Medicine, Yamaguchi University, Yamaguchi, Japan
[e] Tsukuba Primate Research Center, National Institutes of Biomedical Innovation, Health and Nutrition, Tsukuba, Ibaraki 305-0843, Japan

ARTICLE INFO

Keywords:
Coronavirus
Severe acute respiratory syndrome
Nsp4
Viral replication

ABSTRACT

Infection with coronavirus rearranges the host cell membrane to assemble a replication/transcription complex in which replication of the viral genome and transcription of viral mRNA occur. Although coexistence of nsp3 and nsp4 is known to cause membrane rearrangement, the mechanisms underlying the interaction of these two proteins remain unclear. We demonstrated that binding of nsp4 with nsp3 is essential for membrane rearrangement and identified amino acid residues in nsp4 responsible for the interaction with nsp3. In addition, we revealed that the nsp3-nsp4 interaction is not sufficient to induce membrane rearrangement, suggesting the participation of other factors such as host proteins. Finally, we showed that loss of the nsp3-nsp4 interaction eliminated viral replication by using an infectious cDNA clone and replicon system of SARS-CoV. These findings provide clues to the mechanism of the replication/transcription complex assembly of SARS-CoV and could reveal an antiviral target for the treatment of betacoronavirus infection.

1. Introduction

Severe acute respiratory syndrome (SARS) coronavirus (SARS-CoV) is the etiological agent of SARS, an emerging life-threatening disease characterized by high fever, myalgia, nonproductive cough and dyspnea (Booth et al., 2003; Drosten et al., 2003; Ksiazek et al., 2003; Tsang et al., 2003). SARS was first recognized in February 2003, in the midst of a worldwide epidemic that resulted in 8096 patients and 776 deaths, with the last patient being reported in 2004 (de Wit et al., 2016). In 2012, nearly a decade after the SARS epidemic, a novel coronavirus, the Middle East respiratory syndrome (MERS) coronavirus (MERS-CoV), emerged in Saudi Arabia (Zaki et al., 2012) and has since spread to other countries in the Middle East, North Africa, Europe and Asia.

SARS-CoV belongs to the genus *Betacoronavirus* in the family *Coronaviridae*, and is an enveloped virus with a positive-sense and single-stranded RNA genome that has 5'capped and 3' poly (A)-containing 14 open reading frames (ORFs) (Thiel et al., 2003). The genomic size of SARS-CoV is extremely large among RNA viruses and the 5' two-thirds of the genomic RNA has two partially overlapping ORFs, 1a and 1b. Upon infection, the genomic RNA is translated into two large polyproteins and then proteolytically cleaved into 16 mature viral proteins, nsp1 to nsp16 (Prentice et al., 2004; Thiel et al., 2003).

Infection with most of the positive-stranded RNA viruses induces rearrangement of host cell membranes that serve as the platform for a viral replication complex called the replication and transcription complex (RTC) (den Boon and Ahlquist, 2010; Miller and Krijnse-Locker, 2008). The membrane remodeling and consequent RTC formation induced by virus infection are critical for creating a site to support viral RNA synthesis and for protecting newly synthesized RNA from host innate immune systems (den Boon and Ahlquist, 2010). Like infection with other positive-stranded RNA viruses, infection with coronaviruses, including SARS-CoV and murine hepatitis virus (MHV), also induces replication-associated membrane structures, which in the case of betacoronavirus infection consist of two interconnected membrane structures, double-membrane vesicles (DMVs) and convoluted membranes (CMs) (Goldsmith et al., 2004; Gosert et al., 2002; Knoops et al., 2008; Snijder et al., 2006). Furthermore, infection with avian infectious bronchitis virus (IBV) induces a

* Correspondence to: Laboratory of Clinical Research on Infectious Diseases, Research Institute for Microbial Diseases, Osaka University, 3-1 Yamadaoka, Suita-shi, Osaka 565-0871, Japan.
E-mail address: wakamita@biken.osaka-u.ac.jp (W. Kamitani).
[1] These authors contributed equally to this work.

http://dx.doi.org/10.1016/j.virol.2017.07.019
Received 5 June 2017; Received in revised form 9 July 2017; Accepted 14 July 2017

spherular structure derived from the endoplasmic reticulum (ER), which has not been identified in cells infected with other coronavirus species (Maier et al., 2013). Electron microscopy analysis of cells infected with coronavirus reveals that DMVs and CMs localize to the proximity of the ER and partially interconnect with the ER, suggesting that the DMVs and CMs are derived from host ER membranes, despite the lack of canonical ER membrane markers (Gosert et al., 2002; Hagemeijer et al., 2014; Knoops et al., 2008; Snijder et al., 2006; Ulasli et al., 2010).

Among the 16 nsps of coronavirus, nsp3, nsp4, and nsp6 have multiple transmembrane domains (Harcourt et al., 2004; Oostra et al., 2008; Ratia et al., 2008). Although expression of nsp3, nsp4, and nsp6 is observed in RTC upon infection, it is localized in the ER in cells individually expressed by the transfection with expression plasmids (Kanjanahaluethai et al., 2007; Oostra et al., 2008, 2007). In the case of MHV, interaction of nsp4 and the C-terminal one-third of nsp3 (nsp3C) was observed by immunoprecipitation analysis (Hagemeijer et al., 2011), and these proteins were colocalized in the perinuclear foci in cells upon co-transfection with expression plasmids, similar to those observed in infected cells (Hagemeijer et al., 2014, 2011). These data suggest that coexpression of nsp3 and nsp4 results in a membrane rearrangement to induce DMVs and CMs (Hagemeijer et al., 2014). MHV nsp4 is a glycosylated protein, and the glycosylated nsp4 is important for the virus-induced membrane rearrangement and the replication complex function and assembly of DMVs (Clementz et al., 2008; Gadlage et al., 2010). Analyses using confocal and electron microscopy have shown that the expression of nsp3, nsp4, and nsp6 of SARS-CoV induces formation of DMVs in the transfected cells (Angelini et al., 2013). However, limited information is available about the mechanism of interaction between nsp3 and nsp4 of SARS-CoV or the roles of such interaction on viral replication through the formation of membrane rearrangements.

In this study, we demonstrated that the interaction of nsp3 with nsp4 plays a critical role in the replication of SARS-CoV through the rearrangements of host-derived membranes, suggesting that the membrane rearrangement induced by the nsp3-nsp4 interaction is crucial for optimal replication of SARS-CoV.

2. Results

2.1. Co-expression of nsp3C and nsp4 induces redistribution from the ER to concentrated foci in the perinuclear region

In previous reports, co-expression of SARS-CoV nsp4 with the C-terminal one-third of nsp3 (nsp3C) in the cell was shown to redistribute these proteins from the ER to concentrated foci in the perinuclear region (Hagemeijer et al., 2011). To confirm this redistribution of the proteins, we constructed the expression plasmids pCAG nsp4-HA and pCAG nsp3C-3xFLAG carrying an HA-tag and 3xFLAG tag in the C-termini of each protein, respectively (Fig. 1A). Subcellular localization of nsp4 and nsp3C in 293T cells transfected with pCAG nsp4-HA and/or pCAG nsp3C-3xFLAG was determined by immunofluorescence assay (IFA) using anti-HA and anti-FLAG antibodies. Although nsp3C and nsp4 were localized in the ER when expressed individually, both nsp3C and nsp4 were detected in discrete foci in the perinuclear region in cells upon co-expression (Fig. 2A, B top panel), confirming that co-expression of nsp4 with nsp3C of SARS-CoV induces redistribution of the proteins from the ER to concentrated foci in the perinuclear region.

2.2. A large lumenal loop in nsp4 is responsible for induction of the concentrated foci upon co-expression with nsp3C

Amino acid sequences of MHV and SARS-CoV predicted that the nsp4 of both viruses has four transmembrane domains. Previous studies have demonstrated that an nsp4 deletion mutant of MHV lacking the first transmembrane domain did not re-localize upon co-expression with MHV nsp3C (Hagemeijer et al., 2014). To further determine the molecular mechanisms of the interaction between nsp4 and nsp3C of SARS-CoV to induce the perinuclear foci, expression plasmids encoding deletion mutants of nsp4, pCAG nsp4 1-274-HA and pCAG nsp4 1-313-HA (Fig. 1B) were transfected together with pCAG nsp3C-3xFLAG into 293T cells (Fig. 2B 2nd and 3rd panels). Subcellular localization of nsp4 and nsp3C was examined by using anti-HA and anti-FLAG antibodies, respectively, at 30 h posttransfection. Co-expression of nsp3C with nsp4 deletion mutants missing the third and fourth (nsp4 1-313-HA) or second to fourth transmembrane regions (nsp4 1-274-HA) exhibited re-localization to the concentrated foci (Fig. 2B 2nd and 3rd panels), suggesting that the large lumenal loop between the first and second transmembrane regions of nsp4 of SARS-CoV is responsible for induction of the concentrated foci upon co-expression with nsp3C.

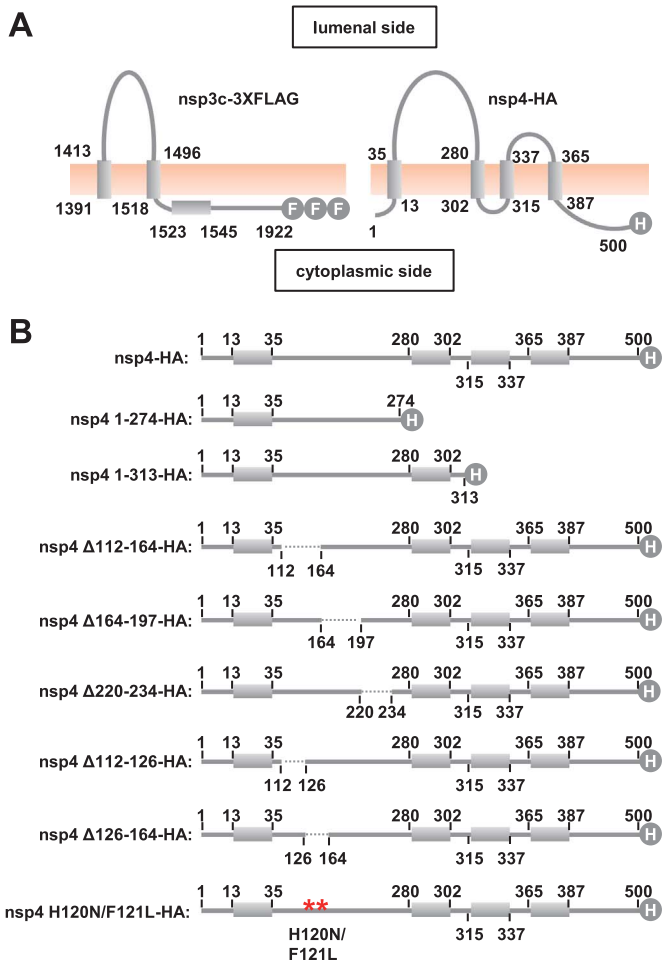

Fig. 1. Schematic diagram of SARS-CoV nsp3C and nsp4 constructs used in this study. (A) Schematic diagrams of the topology of nsp3C and nsp4. SARS-CoV nsp4 is a 500-amino acid protein that has four predicted transmembrane domains. SARS-CoV nsp3 is a 1922-amino acid protein. Nsp3C is the C-terminal region of full-length nsp3. Gray boxes, F, and H represent the transmembrane domain, FLAG-Tag, and HA-Tag, respectively. The numbers indicate amino acid positions. (B) Schematic diagram of the deletion mutants derived from pCAG nsp4-HA. Dashed lines represent deletions. The numbers indicate amino acid positions.

2.3. Two domains in the large lumenal loop of nsp4 are essential for induction of the concentrated foci upon co-expression with nsp3C

To determine the region(s) in the large lumenal loop of SARS-CoV nsp4 responsible for re-localization upon co-expression with nsp3C, expression plasmids encoding deletion in the large lumenal loop of nsp4, pCAG nsp4 Δ112-164-HA, pCAG nsp4 Δ164-197-HA, and pCAG

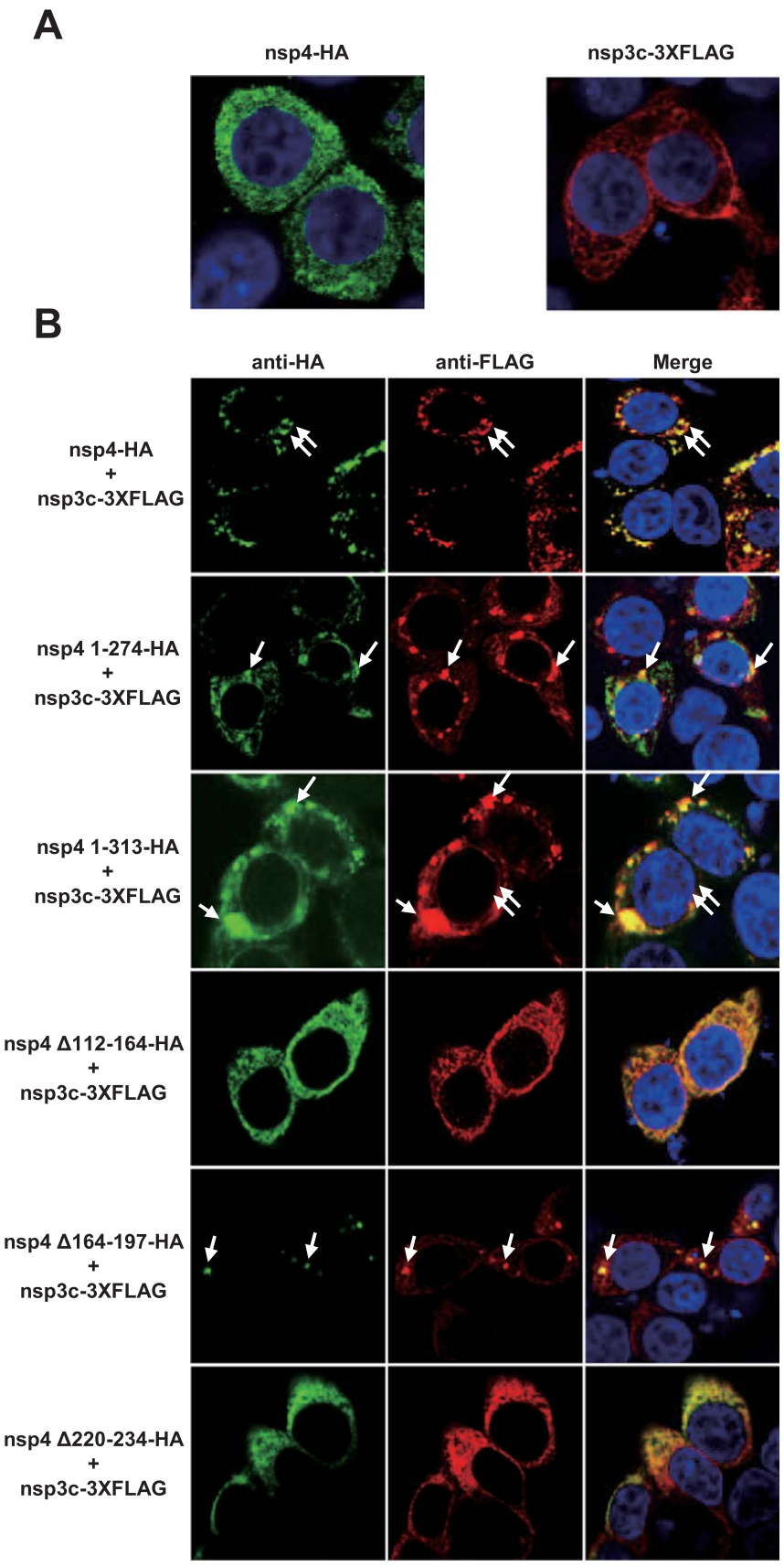

Fig. 2. A large lumenal loop in nsp4 is responsible for the induction of concentrated foci upon co-expression with nsp3C. (A) Intracellular localization of nsp3C or nsp4. 293T cells were transfected with either pCAG nsp3C-3XFLAG or pCAG nsp4-HA and then fixed with 4% PFA at 30 h posttransfection. Nsp3c and nsp4 were stained with rabbit anti-HA antibody and mouse anti-FLAG antibody, followed by CF594-conjugated anti-mouse IgG and CF488-conjugated anti-rabbit IgG, respectively. Cell nuclei were stained with Hoechst 33342. (B) Co-expression of wild type nsp4, nsp4 1-274, nsp4 1-313, nsp4 Δ112-164, nsp4 Δ164-197 or nsp4 Δ220-234 together with nsp3C. At 30 h posttransfection, the cells were fixed with 4% PFA and stained as described above. White arrows represent the concentrated foci.

nsp4 Δ220-234-HA (Fig. 1B) were transfected together with pCAG nsp3C-3xFLAG into 293T cells (Fig. 2B 4th, 5th, and bottom panels). Subcellular localization of nsp4 and nsp3C was examined at 30 h posttransfection. Co-expression of nsp3C with an nsp4 deletion mutant lacking the region from 164 to 197aa but not with mutants lacking the regions from 112 to 164aa or from 220 to 234aa exhibited re-localization to the concentrated foci (Fig. 2B 4th, 5th, and bottom panels), suggesting that the large lumenal loop of SARS-CoV nsp4 has at least two functional domains responsible for induction of the concentrated foci upon co-expression with nsp3C.

2.4. Amino acid residues from positions 112–164 in the large lumenal loop of nsp4 are responsible for binding to nsp3C

To determine the binding region in SARS-CoV nsp4 responsible for the interaction with nsp3C in more detail, 293T cells transfected with either pCAG nsp4 Δ112-164-HA, pCAG nsp4 Δ164-197-HA, or pCAG nsp4 Δ220-234-HA together with pCAG nsp3C-3xFLAG were lysed at 30 h posttransfection and subjected to immunoprecipitation analysis by using anti-HA antibody. The wild type nsp4, nsp4 Δ164-197 and nsp4 Δ220-234 but not nsp4 Δ112-164 were co-immunoprecipitated with nsp3C (Fig. 3A), suggesting that the amino acid residues spanning from 112 to 164 in nsp4 are responsible for binding to nsp3C. To further confirm the binding of nsp4 to nsp3C in situ, a proximity ligation assay (PLA) based on antibodies tagged with a circular DNA probe was performed by using a Duolink® in situ PLA kit (Invitrogen). Once the antibodies are in close proximity, the probes can be ligated together and then amplified with a polymerase. The PLA signals were detected in the cytoplasm of cells co-expressing nsp3C with either wild type nsp4, nsp4 Δ164-197 or nsp4 Δ220-234 but not with nsp4 Δ112-164 at 30 h posttransfection (Fig. 3B), supporting the notion that the amino acid residues from 112 to 164 of SARS-CoV nsp4 are responsible for the interaction with nsp3C. Interestingly, the nsp4 Δ220-234 failed to induce re-localization upon co-expression with nsp3C (Fig. 2B bottom panel), but interaction with nsp3C was detected by using immunoprecipitation and PLA assays (Fig. 3A and B), indicating that the interaction between nsp4 and nsp3C was not sufficient to induce the re-location concentrated foci. These results suggest that another host or viral factor(s) is involved in the re-location concentrated foci induced by interaction between nsp4 and nsp3.

2.5. H120 and F121 in nsp4 are crucial to induce membrane rearrangements

To determine the crucial amino acid residue(s) in SARS-CoV nsp4 required to induce membrane rearrangements through the interaction with nsp3C, we constructed additional expression plasmids encoding deletion mutants of SARS-CoV nsp4, pCAG nsp4 Δ112-126-HA and pCAG nsp4 Δ126-164-HA, as shown in Fig. 1B. Immunoprecipitation analysis showed that the amino acid residues from 112 to 126 in nsp4 are important for binding to nsp3C (Fig. 4A). Moreover, the alignment of amino acid sequences corresponding to the amino acids from 112 to 126 in nsp4 of SARS-CoV revealed that two amino acid residues, H120 and F121, were conserved among betacoronaviruses that included bovine coronavirus (BCoV), MHV, and MERS-CoV (Fig. 4B). Next, to determine the role of H120 and F121 in nsp4 on the interaction with nsp3C, the expression plasmid pCAG nsp4 H120N/F121L-HA, in which H120 and F121 were replaced with N and L, respectively, was co-transfected with pCAG nsp3C-3xFLAG into 293T cells. Immunoprecipitation analysis showed that nsp4 H120N/F121L abrogated binding to nsp3C (Fig. 4A) and IFA showed that nsp4 H120N/F121L lost the ability to re-localize concentrated foci upon co-expression with nsp3C (Fig. 4C). Western blot analysis showed that the amounts of nsp4 H120N/F121L in cells co-transfected with nsp3C were comparable to those of nsp4-wt in co-transfected with nsp3C (Fig. 4D).

To determine the effect of the two amino acid residues, H120 and F121, in SARS-CoV nsp4 on the membrane rearrangements thorough interaction with nsp3C, 293T cells transfected with pCAG nsp4-HA or pCAG nsp4 H120N/F121L-HA together with pCAG nsp3C-3xFLAG at 30 h posttransfection were subjected to transmission electron microscopy (TEM) analysis. TEM analysis revealed that CM-like structures were detected in cells co-expressing nsp3C with nsp4 but not with nsp4 H120N/F121L (Fig. 5A and B). These results suggest that the amino acid residues H120 and F121L in SARS-CoV nsp4 play crucial roles in the membrane remodeling through their interaction with nsp3C.

2.6. A mutant SARS-CoV carrying H120N/F121L substitution in nsp4 exhibits a defect in virus production

To determine the effect of the two amino acid residues, H120 and F121, in SARS-CoV nsp4 on the viral propagation, we generated a mutant virus possessing substitutions of H120 and F121 to N and L,

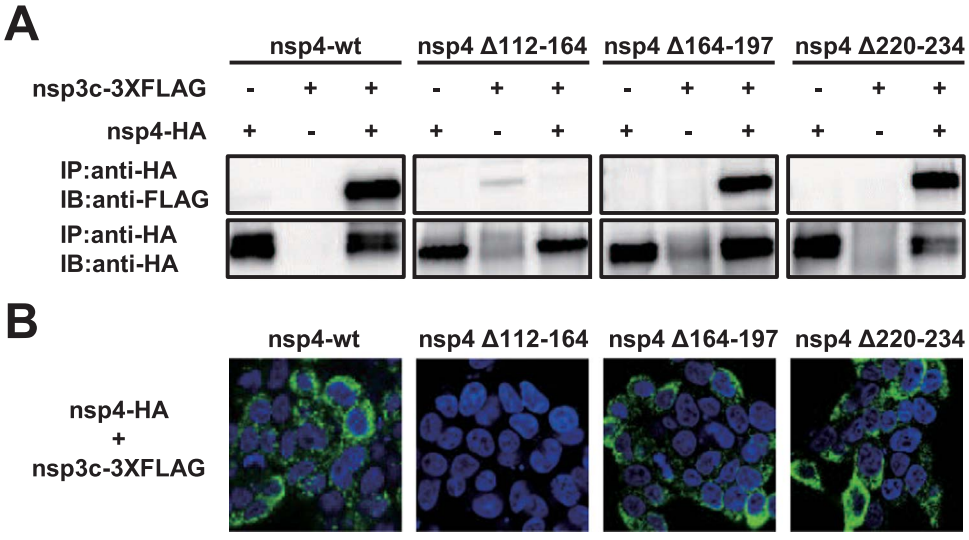

Fig. 3. Amino acid residues from positions 112–164 in the large lumenal loop of nsp4 are responsible for binding to nsp3C. (A) Lysates of 293T cells transfected with pCAG nsp3C-3XFLAG together with the indicated expression plasmids of nsp4 were immunoprecipitated with anti-HA antibody at 30 h posttransfection. The precipitates were subjected to Western blot analysis using anti-FLAG antibody or anti-HA antibody. (B) 293T cells were cotransfected with pCAG nsp3C together with the indicated expression plasmids of nsp4. At 30 h posttransfection, the cells were fixed and subjected to PLA analysis. Cell nuclei were stained with Hoechst 33342.

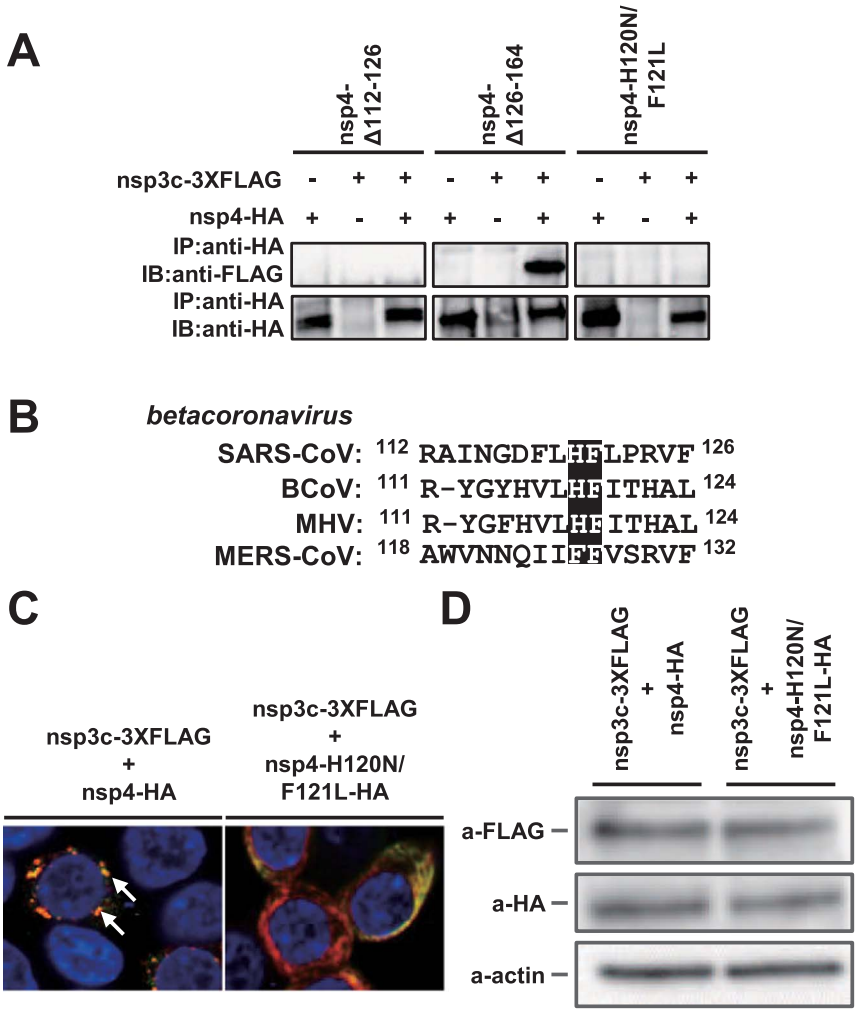

Fig. 4. H120 and F121 in nsp4 are crucial for the induction of concentrated foci and binding with nsp3C. (A) Lysates of 293T cells transfected with pCAG nsp3C-3XFLAG together with the indicated expression plasmids of nsp4 were immunoprecipitated with anti-HA antibody at 30 h posttransfection. The precipitates were subjected to Western blot analysis using anti-FLAG antibody or anti-HA antibody. (B) Sequence alignment of the betacoronavirus nsp4 region from R112 to F126. Nsp4 sequences of the representative betacoronavirus strains were aligned using CLUSTAL W. Completely conserved residues are in black boxes. GenBank accession numbers are as follows: SARS-CoV, AY278741.1; BCoV, NC 003045.1; MHV, FJ647225; MERS-CoV, JX869059.2. (C) 293T cells were cotransfected with pCAG nsp3C-3XFLAG together with either pCAG nsp4-HA or pCAG nsp4 H120N/F121L-HA. At 30 h posttransfection, the cells were fixed and subjected to IFA. Arrows represents the concentrated foci. (D) Lysate of 293T cells transfected with pCAG nsp3C-3XFLAG together with either pCAG nsp4-HA or pCAG nsp4 H120N/F121L-HA were subjected to western blot analysis at 30 h posttransfection.

respectively, by using a reverse genetics system based on the bacterial artificial chromosome (BAC), as described previously (Almazán et al., 2006). Briefly, cDNA of SARS-CoV was assembled in the BAC under the control of the cytomegalovirus immediate-early promoter and flanked at the 3'end by 25-bp of poly(A) followed by an HDV ribozyme and a BGH termination sequence (Almazán et al., 2006), and designated pBAC-SARS-wt. A mutant clone, pBAC-SARS-H120N/F121L, was generated by introducing an H120N/F121L substitution in nsp4 into the parental pBAC-SARS-wt (Fig. 6A). To determine the effect of H120N/F121L mutation in nsp4 on the infectious particle formation and viral RNA replication of SARS-CoV, infectious titers in the culture supernatants and intracellular viral RNA in Huh7 cells transfected with either pBAC-SARS-wt or pBAC-SARS-H120N/F121L were determined at 72 h posttransfection (Fig. 6B). Although the infectious titers in the supernatants reached 5.62E+04 TCID50/ml and the amounts of viral RNA determined by real-time PCR were increased in a time-dependent manner in cells transfected with pBAC-SARS-wt, no infectious titer in the supernatants and no replication of intracellular viral RNA was detected in those transfected with pBAC-SARS-H120N/F121L (Fig. 6C and D). These results suggest that the amino acid residues H120 and F121 in nsp4 play an important role in viral RNA replication through the membrane remodeling.

Next, to confirm the importance of H120 and F121 in nsp4 on the replication of SARS-CoV, we inserted a reporter gene into pBAC-SARS-H120N/F121L. Briefly, the accessory gene 7ab in pBAC-SARS-H120N/F121L was replaced with renilla luciferase and firefly luciferase genes by using a Red/ET Recombination System Counter-Selection BAC MODIFICATION Kit, to obtain pBAC-SARS-H120N/F121L-rluc and pBAC-SARS-H120N/F121L-fluc, respectively (Fig. 6E). As a control, pBAC-SARS-wt-fluc, in which the 7ab gene was replaced with a firefly luciferase gene, was generated. pBAC-SARS-H120N/F121L-rluc was transfected into 293T cells together with either pBAC-SARS-wt-fluc or pBAC-SARS-H120N/F121L-fluc, and the luciferase activities in cell lysates were determined at 24 h posttransfection (Fig. 6F). The expressions of renilla luciferase and firefly luciferase were detected in cells transfected with pBAC-SARS-H120N/F121L-rluc together with pBAC-SARS-wt-fluc but not with pBAC-SARS-H120N/F121L-fluc (Fig. 6G). These results suggest that propagation of the replication-deficient mutant SARS-CoV possessing a substitution of H120N/F121L in nsp4 was rescued by the co-infection with a wild type SARS-CoV.

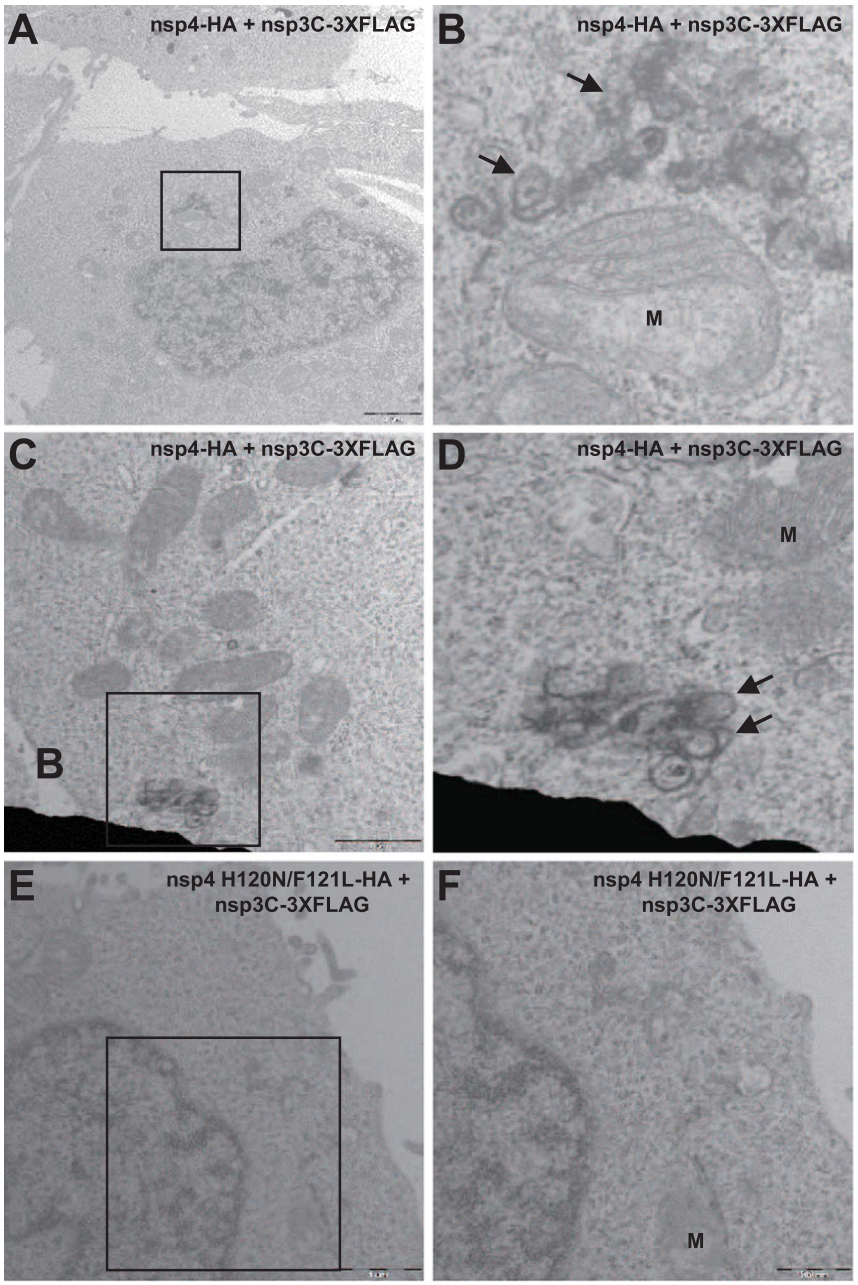

Fig. 5. H120 and F121 in nsp4 are crucial for the induction of the membrane rearrangements. 293T cells were co-transfected with pCAG nsp3C-3XFLAG together with either pCAG nsp4-HA or pCAG nsp4 H120N/F121L-HA. At 30 h posttransfection, the cells were fixed and subjected to TEM analysis. Boxes in the left images represent area of magnification in right image. Black arrows represent CM-like structures. M, mitochondria.

2.7. A mutant SARS-CoV replicon carrying H120N/F121L substitutions in nsp4 exhibits a defect in the replication of viral RNA

To determine the biological significance, with respect to viral RNA replication, of the membrane remodeling induced by the interaction of nsp4 with nsp3C, we employed an RNA replicon system in which SARS-CoV RNA replicates but does not produce any infectious particles, as described previously (Almazán et al., 2006; Tanaka et al., 2012). We introduced H120N/F121L mutations in nsp4 of the parental replicon, pBAC-SARS-Rep-wt, to generate pBAC-SARS-Rep-H120N/F121L (Fig. 7A). As a negative control, we generated pBAC-SARS-Rep-SAD carrying a mutation in nsp12 deficient in RNA-dependent RNA polymerase activity by the replacement of D760 to A760 (Subissi et al., 2014) (Fig. 7A). Northern blot analysis of 293T cells at 24 h and 36 h posttransfection with pBAC-SARS-Rep-wt, pBAC-SARS-Rep-SAD or pBAC-SARS-Rep-H120N/F121L using an N gene-specific probe revealed that no mRNA was detected in cells transfected with either pBAC-SARS-Rep-H120N/F121L or pBAC-SARS-Rep-SAD, in contrast to those transfected with pBAC-SARS-Rep-wt (Fig. 7B). To further confirm the impairment of replication of the replicon carrying mutations in H120 and F121, the levels of renilla luciferase in 293T cells transfected with pBAC-SARS-Rep-wt, pBAC-SARS-Rep-SAD or pBAC-SARS-Rep-H120N/F121L were determined at 24 h and 36 h posttransfection. As we expected, expression of renilla luciferase was detected in cells transfected with pBAC-SARS-Rep-wt, but not in those with pBAC-SARS-Rep-H120N/F121L or pBAC-SARSRep-SAD (Fig. 7C), suggesting that both H120 and F121 in SARS-CoV nsp4 play critical roles in the viral replication by remodeling the membrane through binding with nsp3.

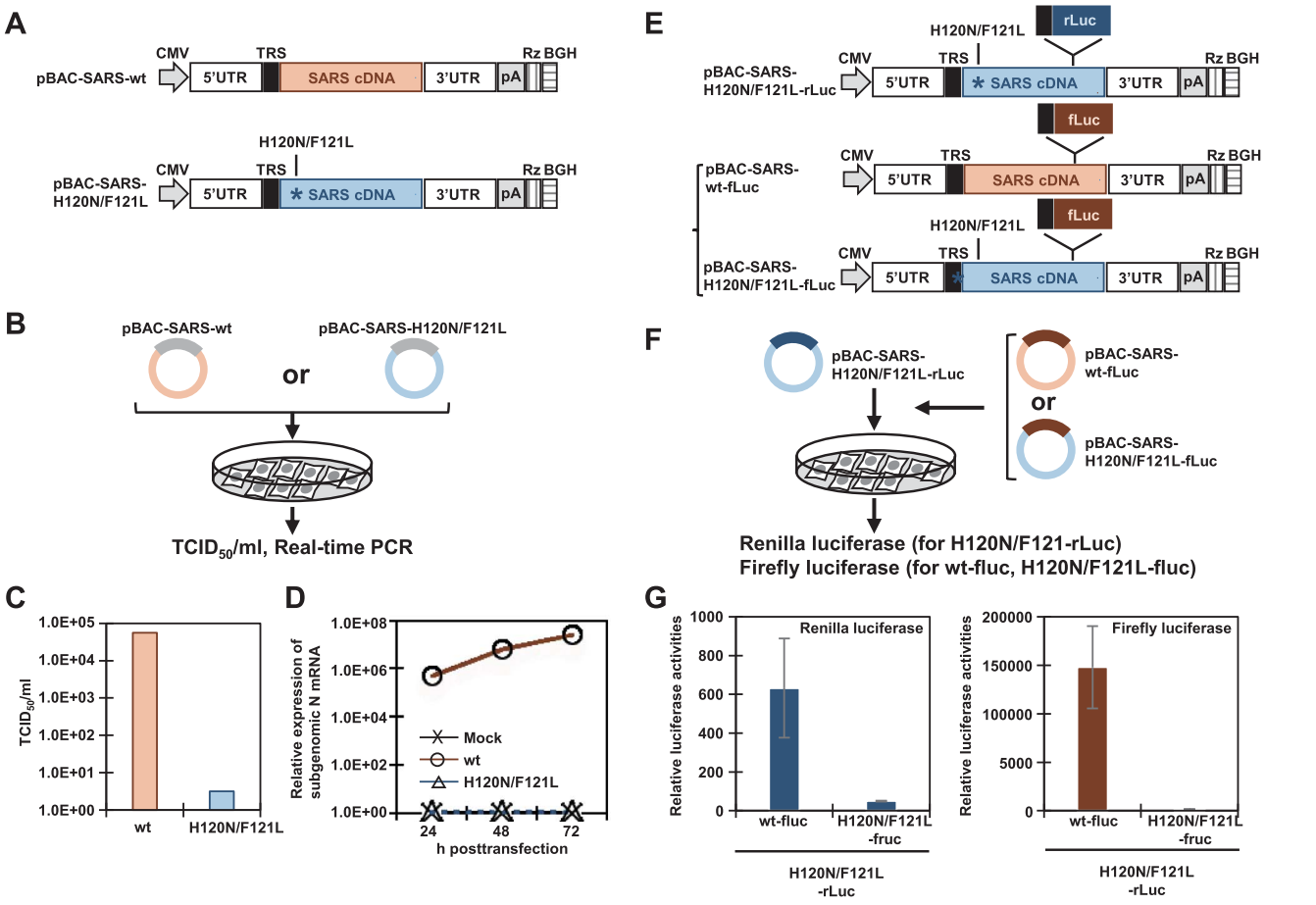

Fig. 6. A mutant SARS-CoV carrying H120N/F121L substitution in nsp4 exhibits defects in virus production. (A) Schematic diagram of infectious cDNAs of SARS-CoV. CMV, CMV promoter; TRS, transcription-regulatory sequence of SARS-CoV; pA, synthetic poly(A) tail; Rz, the self-cleaving ribozyme of hepatitis delta virus; BGH, BGH termination and polyadenylation signals. An asterisk represents the position of mutated amino acids. (B) Scheme for recovery of recombinant infectious viruses. Huh7 cells were transfected with either pBAC-SARS-wt (wt) or pBAC-SARS-H120N/F121L (H120N/F121L). At 72 h posttransfection, the culture supernatants were harvested, and infectious titers were determined by $TCID_{50}$ assays in Vero cells (C). The expression of subgenomic N mRNA was determined at 24, 36, and 72 h posttransfection by using real-time PCR (D). The relative abundance of subgenomic N mRNA was normalized to an endogenous GAPDH mRNA. (E) Schematic diagram of infectious cDNAs carrying the luciferase gene of SARS-CoV. CMV, CMV promoter; rLuc, renilla luciferase; fLuc, firefly luciferase. The black boxes and asterisks represent TRS and the positions of mutated amino acids, respectively. (F) Schematic diagram of recovery experiment. pBAC-SARS-H120N/F121L-rluc was transfected into 293T cells together with either pBAC-SARS-wt-fluc or pBAC-SARS-H120N/F121L-fluc (G) 293T cells were transfected with pBAC-SARS-H120N/F121L-rLuc together with either pBAC-SARS-wt-fLuc or pBAC-SARS-H120N/F121L-fLuc. Renilla luciferase (left panel) and firefly luciferase (right panel) activities in the cells were determined at 24 h posttransfection. The values represent the means ± SD from three independent experiments.

3. Discussion

Like other positive-strand RNA viruses, coronaviruses induce a variety of membrane rearrangement structures (Goldsmith et al., 2004; Gosert et al., 2002; Snijder et al., 2006), including the DMVs and CMs that serve as a scaffold for replication/transcription complexes (Hagemeijer et al., 2014; Maier et al., 2013). Upon SARS-CoV infection, viral RNA is translated into 16 mature viral proteins, nsp1 to nsp16, by processing with two viral proteinases (Prentice et al., 2004), and some of them localize to DMVs and CMs (Knoops et al., 2008). In SARS-CoV, nsp3, nsp4 and nsp6 contain multiple hydrophobic and membrane-spanning domains (Hagemeijer et al., 2014), and co-expression of nsp3, nsp4 and nsp6 was shown to result in the formation of DMVs and CMs (Angelini et al., 2013). In addition, Hagemeijer et al. showed that co-expression of nsp4 with the C-terminal one-third of nsp3 re-translocates both proteins into concentrated foci that predominantly localize in the perinuclear region (Hagemeijer et al., 2011). Further, the large lumenal loop between the first and second transmembrane domains of MHV nsp4 was shown to be essential for the induction of membrane rearrangement (Hagemeijer et al., 2014). Although many studies have investigated the role of the co-expression of nsp3 and nsp4 in inducing host membrane rearrangement the molecular mechanisms underlying the interaction of nsp3 with nsp4 and the role of this interaction in viral replication are largely unknown. In the present study, we identified the crucial amino acid residues in nsp4 responsible for the interaction with nsp3 and demonstrated that the membrane rearrangement induced by the interaction of nsp3 with nsp4 is crucial for formation of viral replication complexes. We also showed by means of immunoprecipitation and PLA assays that the amino acids residues from positions 112–164 and from 220 to 234 of nsp4 are critical for the induction of membrane rearrangement upon co-expression with nsp3, and the amino acids residues from positions 112–164 of nsp4 form the binding site with nsp3.

Sparks et al. demonstrated that both the first and second lumenal loops of nsp4 are critical for viral replication by using an MHV infectious clone (Sparks et al., 2007). Although the second lumenal loop of nsp4 does not participate in the membrane rearrangement (Hagemeijer et al., 2014), the role of the lumenal loops in the viral replication is still unclear. The roles of the glycosylation in the first lumenal loop of nsp4 on the membrane rearrangement have been well studied. MHV has two glycosylation sites (N176 and N237) and SARS-CoV has one glycosylation site (N131) (Clementz et al., 2008; Gadlage et al., 2010; Oostra et al., 2008). Interestingly, morphologically aberrant DMVs were observed in cells upon infection with a mutant MHV possessing nsp4 with no glycosylation site and RNA replication

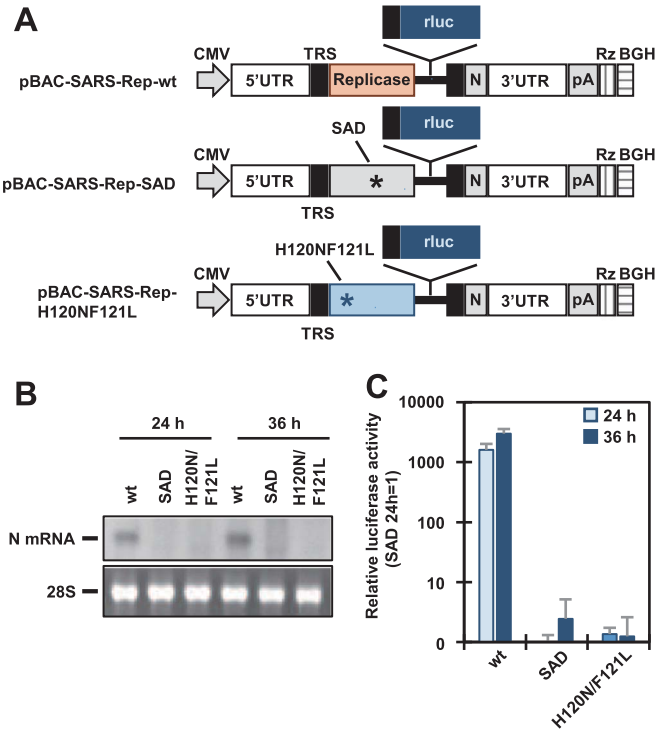

Fig. 7. A mutant SARS-CoV replicon carrying H120N/F121L substitution in nsp4 exhibits defects in viral genome replication. (A) Schematic diagram of cDNAs of the RNA replicon of SARS-CoV. CMV, CMV promoter; TRS, transcription-regulatory sequence of SARS-CoV; pA, synthetic poly(A) tail; Rz, the self-cleaving ribozyme of hepatitis delta virus; BGH, BGH termination and polyadenylation signals; rLuc, renilla luciferase; fLuc, firefly luciferase. Black boxes and asterisks represent TRS and the positions of mutated amino acids, respectively. (B) 293T cells were transfected with pBAC-SARS-Rep-wt (wt), pBAC-SARS-Rep-SAD (SAD) or pBAC-SARS-Rep-H120N/F121L (H120N/F121L), and the expression of viral RNA was determined at 24 h and 36 h posttransfection. Total RNAs extracted from the cells were subjected to Northern blot analysis using a riboprobe for the N gene. 28S rRNA was stained with ethidium bromide. (C) Luciferase activities in 293T cells transfected with pBAC-SARS-Rep-wt (wt), pBAC-SARS-Rep-SAD (SAD) or pBAC-SARS-Rep-H120N/F121L (H120N/F121L) were determined at 24 h and 36 h posttransfection. The values represent the means ± SD from three independent experiments.

was impaired (Beachboard et al., 2015; Gadlage et al., 2010). Although we did not examine the effect of mutation of N131 in nsp4 on the membrane rearrangement and viral propagation in this study, the H120N/F121L mutations in nsp4, which are distant from the N131 glycosylation site, induced a complete loss of membrane rearrangement and impairment of viral RNA replication, suggesting that the specific interaction of nsp4 with nsp3 plays roles in viral replication.

In addition, substitution of the conserved cysteine residues to serine affected the membrane rearrangement of MHV nsp4 (Hagemeijer et al., 2014). Although we did not focus on the cysteine residues in SARS-CoV nsp4 in this study, we did note that three cysteines between 220 and 234 were well conserved in coronaviruses including MHV, SARS-CoV and coronaviruses in other genera. Because nsp4 Δ 220–234 was capable of binding to nsp3c, the nsp4-nsp3 interaction is likely independent of cysteine-mediated interaction. Further studies are needed to understand the role of the cysteine residues in nsp4 of SARS-CoV on viral replication.

Many viruses utilize host factors that are involved in the intracellular transport of virus-induced vesicles (den Boon and Ahlquist, 2010; Miller and Krijnse-Locker, 2008). The vesicle coat proteins known as COPII proteins transport proteins from the rough ER to the Golgi apparatus, and are involved in the production of vesicles in cells infected with poliovirus (PV) (Rust et al., 2001). ADP-ribosylation factors, which play a role in the regulation of membrane dynamics and protein transport, are localized to the PV-induced membranes in cells infected with PV (Belov et al., 2007). Vesicle-associated-membrane protein-associated proteins (VAPs) remodel the ER by interacting with NIR2 to mediate formation of HCV-induced membranes (Moriishi and Matsuura, 2007). Although the precise interaction of the coronavirus RTC with host proteins is largely unknown, ERAD tuning pathway is suggested to be involved in the RTC formation of MHV (Hagemeijer et al., 2014; Reggiori et al., 2010), since RTC proteins coexist with the ERAD regulator proteins EDEM1 and OS9, and the ERAD machinery mediated by ERAD regulator proteins participates in the formation of LC3-I-positive RTC (Noack et al., 2014; Reggiori et al., 2010). In this study, we found that the nsp4 mutant lacking the amino acid residues from positions 220–234 is capable of binding to nsp3C but lacks induction of re-localization (Fig. 3 and 4) and membrane rearrangement (Fig. 5), suggesting that other host or viral factor(s), such as EDEM1 and OS9, participate in the membrane rearrangement induced by the interaction between nsp4 and nsp3.

In addition, we identified two amino acids residues (H120 and F121) in nsp4 that are well conserved among betacoronaviruses, including MERS-CoV, but not among alphacoronaviruses or gammacoronaviruses. These residues were essential for the membrane rearrangements induced by the interaction with nsp3, suggesting that the mode of interaction of nsp4 with nsp3 differs among the different types of coronaviruses. In fact, cells infected with infectious bronchitis virus (IBV), which belongs to *gammacoronavirus*, induce structures called zippered ER and spherules in addition to DMVs (Maier et al., 2013). Such morphological difference of virus-induced membrane structures among coronaviruses may be due to functional and structural difference of nsp3 and nsp4. Further studies will be needed to elucidate the mode of interaction of nsp4 with nsp3 differs among the different types of coronaviruses.

RNA replicon and infectious cDNA carrying the replacement of H120N/F121L in nsp4 were lethal, suggesting that nsp3-nsp4 binding and induction of the membrane rearrangements correlates with viral propagation. Moreover, we showed that co-infection with a wild type virus rescued the replication of the replication-deficient SARS-CoV carrying a mutation in nsp4, suggesting that the membrane rearrangements inducing by the nsp3-nsp4 interaction are necessary to provide a site for the viral genome replication. Two cysteine proteases, nsp3 and nsp5 of SARS-CoV, participate in processing of the polyprotein to release other nsps, and chemical compounds that have been shown to suppress the proteinase activities (Konno et al., 2016; Ratia et al., 2008; Thanigaimalai et al., 2013).

Therefore, while further studies will be needed to elucidate the molecular mechanisms underlying nsp4-mediated membrane rearrangements, our data provide important information about a function of such rearrangements—namely, the nsp4 mutations H120N and F121L impair viral RNA replication by impairing the membrane rearrangements. Therefore, interventions to block the interaction of nsp4 with host or viral proteins might be a novel target for the development of antivirals for betacoronaviruses.

4. Materials & methods

4.1. Cells and transfection

Cultures of 293T (human kidney), BHK-21 (hamster kidney), Huh7 (human hepatocellular carcinoma) and VeroE6 (monkey kidney) cells were maintained in Dulbecco's modified minimum essential medium (DMEM) (Nacalai Tesque, Kyoto, Japan) containing 10% heat-inactivated fetal bovine serum (FBS), 100 U/ml penicillin, and 100 mg/ml streptomycin. All cells were cultured in a humidified 5% CO2 atmosphere at 37 °C. The plasmids were transfected into 293T cells by use of polyethyleneimine (PEI) (Polysciences, Warrington, PA). At 4 h post-transfection, the media were replaced with fresh DMEM containing 10% FBS.

4.2. Plasmid constructions

The PCR products of SARS-CoV nsp3C with a c-terminal 3×FLAG-tag sequence and SARS-CoV nsp4 with a c-terminal HA-tag sequence were cloned into pCAGGS-MCS, yielding pCAG nsp3C-3×FLAG and pCAG nsp4-HA, respectively. An inverse PCR procedure using pCAG nsp4-HA as the template was employed to generate pCAG nsp4Δ220-234-HA, pCAG nsp4Δ164-197-HA, pCAG nsp4 Δ112-164-HA, and pCAG nsp4 H121N/F122L-HA by using a KOD mutagenesis kit (Toyobo, Osaka, Japan). The sequences of all of the constructs were confirmed with an ABI PRISM 3100 genetic analyzer (Applied Biosystems, Tokyo, Japan).

4.3. Indirect immunofluorescence assay

293T Cells cultured on poly-L-lysine (PLL)-coated glass bottom dishs (Matsunami Glass Ind. Ltd., Osaka, Japan) were cotransfected with pCAG nsp3C-3×FLAG together with the indicated expression plasmids of nsp4. At 30 h posttransfection, the cells were fixed with 4% paraformaldehyde in phosphate-buffered saline (PBS) for 30 min at 4 °C. After washing one time with PBS, the cells were permeabilized for 15 min at room temperature with PBS containing 0.1% Tween-20. The cells were then incubated with a mixture of rabbit anti-HA antibody (1:300; MBL, Aichi, Japan) and mouse anti-DYKDDDDK (FLAG) antibody (1:300; Wako, Osaka, Japan) for 1 h at RT, washed three times with PBS, and incubated with a mixture of CF488-conjugated anti-rabbit IgG (1:500; Sigma, St. Louis, MO), CF594-conjugated anti-mouse IgG (1:500; Sigma), and Hoechst 33342 (Dojindo, Kumamoto, Japan) for 1 h at RT. Finally, the cells were washed three times with PBS and observed with a FluoView FV1000 laser scanning confocal microscope (Olympus, Tokyo, Japan).

4.4. Immunoprecipitation assay

293T cells were cotransfected with pCAG nsp3-3×FLAG together with the indicated expression plasmids of nsp4. At 32 h posttransfection, the cells were lysed with lysis buffer (10 mM HEPES, pH 7.4, containing 150 mM NaCl and 0.5% TritonX-100). The cell lysates were incubated with mouse anti-HA antibody (Covance, Richmond, CA) for 1 h at 4 °C, and the immunoprecipitates were collected by centrifugation after incubation with protein A/G PLUS-Agarose (Santa Cruz Biotechnology, Santa Cruz, CA) for 1 h at 4 °C. The immunoprecipitates were incubated for 15 min at 42 °C in Laemmli sample buffer and then subjected to sodium dodecyl sulfate polyacrylamide gel electrophoresis. The proteins were transferred to polyvinylidene difluoride membranes (Millipore, Bedford, MA) and then incubated with rabbit anti-HA antibody (1:2000; MBL) or rabbit anti-FLAG antibody (1:2000; MBL) for 16 h at 4 °C. After washing three times, the membranes were incubated with horseradish peroxidase (HRP)-conjugated anti-rabbit IgG (Sigma) for 1 h at RT. The immunocomplexes were visualized with Chemi-Lumi One Ultra (Nacalai Tesque) and detected by using LAS-4000EPUV (Fujifilm, Tokyo, Japan).

4.5. In situ proximity ligation assay

293T cells were cultured on PLL-coated glass bottom dishs, cotransfected with pCAG nsp3C-3×FLAG together with the indicated expression plasmids of nsp4, fixed with 4% PFA in PBS, permeabilized with PBS containing 0.1% Tween-20, and then incubated with primary antibodies as described above. An in situ proximity ligation assay (PLA) was performed using a Duolink® in situ PLA kit (Invitrogen, Carlsbad, CA) according to the manufacturer's instructions. Briefly, after washing three times, the samples were incubated with anti-mouse PLUS (Invitrogen) and anti-rabbit MINUS (Invitrogen) for 1 h at RT. After washing two times, a ligase solution (Invitrogen) was applied for 30 min at 37 °C. The samples were washed and a mixture of amplification Green solution (Invitrogen) and polymerase solution (Invitrogen) was applied for 1 h at 37 °C. The samples were then washed a final time, mounted using Mounting Medium with DAPI (Invitrogen) and examined with a FluoView FV1000 laser scanning confocal microscope (Olympus).

4.6. Transmission electron microscopy (TEM) analysis

293T cells were cultured on a gridded glass bottom dish (MatTek, Ashland, MA) and transfected with pCAG nsp4-HA and pCAG nsp3c-3×FLAG as described above. At 30 h posttransfection, the cells were fixed with 2.5% glutaraldehyde in 0.1 M cacodylate buffer (pH 7.4) containing 7% sucrose. The cells were postfixed for 1 h with 1% osmium tetroxide and 0.5% potassium ferrocyanide in 0.1 M cacodylate buffer (pH 7.4), dehydrated in a graded series of ethanol, and embedded in Epon812 (TAAB, Reading, UK). Ultrathin (80 nm) sections were stained with saturated uranyl acetate and lead citrate solution. Electron micrographs were obtained with a JEM-1011 transmission electron microscope (JEOL, Tokyo, Japan).

4.7. Generation of infectious recombinant SARS-CoV

The BAC clone carrying a full-length infectious genome of the Urbani strain of SARS-CoV, pBAC-SARS-wt, was generated according to a previously report (Almazán et al., 2006). The BAC DNA of SARS-CoV-Rep, which was kindly provided by Luis Enjuanes, was used as a backbone BAC sequence to generate pBAC-SARS-wt. The BAC infectious clone carrying two amino acid substitutions, H120N and F121L, in nsp4 was generated by modification of the pBAC-SARS-wt as a template using a Red/ET Recombination System Counter-Selection BAC Modification Kit (Gene Bridges, Heidelberg, Germany), yielding pBAC-SARS-H120N/F121N. The sequences of the two introduced mutations were confirmed as described above. The recombinant viruses were recovered according to established protocols, as described previously (Almazán et al., 2006).

4.8. Virus titration

Virus infectivity was determined by a 50% tissue culture infectious dose ($TCID_{50}$) TCID50 assay with Vero cells. Briefly, the viruses were serially diluted and inoculated onto monolayers of Vero cells. After 1 h of absorption, the cells were washed with serum-free DMEM and cultured in DMEM containing 1% FBS. At 72 h postinfection, cells were fixed with 10% formaldehyde neutral buffer solution, and $TCID_{50}$_ was calculated by the Spearman and Karber algorithm.

4.9. Real-time PCR

Total RNA was prepared from cells by using a PureLink RNeasy mini kit (ThermoFisher Scientific), and first-strand cDNA was synthesized using a ReverTra Ace qPCR RT kit (TOYOBO). The level of each cDNA was determined by using Thunderbird SYBR qPCR Mix (TOYOBO), and fluorescent signals were analyzed by using an ABI Prism 7000 system (Applied Biosystems). The SARS-CoV N and GAPDH genes were amplified using the following primer pairs: 5'-tgggtccaccaaatgtaatgc -3' and 5'- aagccaaccaacctcgatctc -3' for SARS-CoV N and 5'-gaaggtgaaggtcggagt-3' and 5'-gaagatggtgatgggatttc3' for GAPDH. The value of SARS-CoV N mRNA was normalized to that of GADH mRNA.

4.10. SARS-CoV replicon assay

The construction of the SARS-CoV-derived replicon carrying a renilla luciferase reporter gene (rluc), pBAC-SARS-Rep-wt (previously referred to as pBACwt-rluc), has been described elsewhere (Almazán et al., 2006; Tanaka et al., 2012). The BAC DNA of SARS-CoV-Rep,

which was kindly provided by Luis Enjuanes, was used as a backbone BAC sequence to generate pBAC-wtrluc. A Red/ET Recombination System Counter-Selection BAC Modification Kit (Gene Bridges) was used to generate mutations (H120N and F121L) in nsp4 and a mutation (D760A) in nsp12 by using pBAC-SARS-Rep-wt as a template, yielding pBAC-SARS-Rep-H120N/F121L and pBAC-SARS-Rep-SAD. The sequences of the two introduced mutations were confirmed with an ABI PRISM 3100 genetic analyzer, as described above. Lysates of 293T cells transfected with the indicated BAC DNA were lysed with passive lysis buffer (Promega). Luciferase activity was determined by using a dual-luciferase assay system (Promega, Madison, WI) and an AB-2200 luminometer (Atto, Tokyo, Japan).

4.11. Northern blot analysis

Northern blot analysis was performed by using total intracellular RNAs as described previously (Tanaka et al., 2012), and visualization was performed using a digoxigenin (DIG) luminescence detection kit (Roche).

Acknowledgments

We thank Ms. Kaede Yukawa for secretarial assistance, Ms. Kanako Yoshizawa for technical assistance, Dr. Shinji Makino (University of Texas Medical Branch) for helpful insights, Drs. Makoto Sugiyama and Naoto Ito (Gifu University) for kindly providing research reagents, and Drs. Luis Enjuanes and Marta L. DeDiego for kindly providing a SARS-CoV-Rep. WK was supported by a Grant-in-Aid for Scientific Research (16K08811) and by funds from the Takeda Science Foundation.

References

Almazán, F., Dediego, M.L., Galán, C., Escors, D., Alvarez, E., Ortego, J., Sola, I., Zuñiga, S., Alonso, S., Moreno, J.L., Nogales, A., Capiscol, C., Enjuanes, L., 2006. Construction of a severe acute respiratory syndrome coronavirus infectious cDNA clone and a replicon to study coronavirus RNA synthesis. J. Virol. 80, 10900–10906.

Angelini, M.M., Akhlaghpour, M., Neuman, B.W., Buchmeier, M.J., 2013. Severe acute respiratory syndrome coronavirus nonstructural proteins 3, 4, and 6 induce double-membrane vesicles. MBio 4, 1–10.

Beachboard, D.C., Anderson-Daniels, J.M., Denison, M.R., 2015. Mutations across murine hepatitis virus nsp4 alter virus fitness and membrane modifications. J. Virol. 89, 2080–2089.

Belov, G.A., Altan-Bonnet, N., Kovtunovych, G., Jackson, C.L., Lippincott-Schwartz, J., Ehrenfeld, E., 2007. Hijacking components of the cellular secretory pathway for replication of poliovirus RNA. J. Virol. 81, 558–567.

Booth, C.M., Matukas, L.M., Tomlinson, G.A., Rachlis, A.R., Rose, D.B., Dwosh, H.A., Walmsley, S.L., Mazzulli, T., Avendano, M., Derkach, P., Ephtimios, I.E., Kitai, I., Mederski, B.D., Shadowitz, S.B., Gold, W.L., Hawryluck, L.A., Rea, E., Chenkin, J.S., Cescon, D.W., Poutanen, S.M., Detsky, A.S., 2003. Clinical features and short-term outcomes of 144 patients with SARS in the greater Toronto area. JAMA 289, 2801–2809.

Clementz, M.A., Kanjanahaluethai, A., O'Brien, T.E., Baker, S.C., 2008. Mutation in murine coronavirus replication protein nsp4 alters assembly of double membrane vesicles. Virology 375, 118–129.

de Wit, E., van Doremalen, N., Falzarano, D., Munster, V.J., 2016. SARS and MERS: recent insights into emerging coronaviruses. Nat. Rev. Microbiol. 14, 523–534.

den Boon, J.A., Ahlquist, P., 2010. Organelle-like membrane compartmentalization of positive-strand RNA virus replication factories. Annu. Rev. Microbiol. 64, 241–256.

Drosten, C., Gunther, S., Preiser, W., van der Werf, S., Brodt, H.R., Becker, S., Rabenau, H., Panning, M., Kolesnikova, L., Fouchier, R.A., Berger, A., Burguiere, A.M., Cinatl, J., Eickmann, M., Escriou, N., Grywna, K., Kramme, S., Manuguerra, J.C., Muller, S., Rickerts, V., Sturmer, M., Vieth, S., Klenk, H.D., Osterhaus, A.D., Schmitz, H., Doerr, H.W., 2003. Identification of a novel coronavirus in patients with severe acute respiratory syndrome. N. Engl. J. Med. 348, 1967–1976.

Gadlage, M.J., Sparks, J.S., Beachboard, D.C., Cox, R.G., Doyle, J.D., Stobart, C.C., Denison, M.R., 2010. Murine hepatitis virus nonstructural protein 4 regulates virus-induced membrane modifications and replication complex function. J. Virol. 84, 280–290.

Goldsmith, C.S., Tatti, K.M., Ksiazek, T.G., Rollin, P.E., Comer, J.A., Lee, W.W., Rota, P.A., Bankamp, B., Bellini, W.J., Zaki, S.R., 2004. Ultrastructural characterization of SARS coronavirus. Emerg. Infect. Dis. 10, 320–326.

Gosert, R., Kanjanahaluethai, A., Egger, D., Bienz, K., Baker, S.C., 2002. RNA replication of mouse hepatitis virus takes place at double-membrane vesicles. J. Virol. 76, 3697–3708.

Hagemeijer, M.C., Monastyrska, I., Griffith, J., van der Sluijs, P., Voortman, J., van Bergen en Henegouwen, P.M., Vonk, A.M., Rottier, P.J., Reggiori, F., de Haan, C.A., 2014. Membrane rearrangements mediated by coronavirus nonstructural proteins 3 and 4. Virology 458–459, 125–135.

Hagemeijer, M.C., Ulasli, M., Vonk, A.M., Reggiori, F., Rottier, P.J., de Haan, C.A., 2011. Mobility and interactions of coronavirus nonstructural protein 4. J. Virol. 85, 4572–4577.

Harcourt, B.H., Jukneliene, D., Kanjanahaluethai, A., Bechill, J., Severson, K.M., Smith, C.M., Rota, P.A., Baker, S.C., 2004. Identification of severe acute respiratory syndrome coronavirus replicase products and characterization of papain-like protease activity. J. Virol. 78, 13600–13612.

Kanjanahaluethai, A., Chen, Z., Jukneliene, D., Baker, S.C., 2007. Membrane topology of murine coronavirus replicase nonstructural protein 3. Virology 361, 391–401.

Knoops, K., Kikkert, M., Worm, S.H., Zevenhoven-Dobbe, J.C., van der Meer, Y., Koster, A.J., Mommaas, A.M., Snijder, E.J., 2008. SARS-coronavirus replication is supported by a reticulovesicular network of modified endoplasmic reticulum. PLoS Biol. 6, e226.

Konno, H., Wakabayashi, M., Takanuma, D., Saito, Y., Akaji, K., 2016. Design and synthesis of a series of serine derivatives as small molecule inhibitors of the SARS coronavirus 3CL protease. Bioorg. Med. Chem. 24, 1241–1254.

Ksiazek, T.G., Erdman, D., Goldsmith, C.S., Zaki, S.R., Peret, T., Emery, S., Tong, S., Urbani, C., Comer, J.A., Lim, W., Rollin, P.E., Dowell, S.F., Ling, A.E., Humphrey, C.D., Shieh, W.J., Guarner, J., Paddock, C.D., Rota, P., Fields, B., DeRisi, J., Yang, J.Y., Cox, N., Hughes, J.M., LeDuc, J.W., Bellini, W.J., Anderson, L.J., Group, S.W., 2003. A novel coronavirus associated with severe acute respiratory syndrome. N. Engl. J. Med. 348, 1953–1966.

Maier, H.J., Hawes, P.C., Cottam, E.M., Mantell, J., Verkade, P., Monaghan, P., Wileman, T., Britton, P., 2013. Infectious bronchitis virus generates spherules from zippered endoplasmic reticulum membranes. MBio 4, e00801–e00813.

Miller, S., Krijnse-Locker, J., 2008. Modification of intracellular membrane structures for virus replication. Nat. Rev. Microbiol. 6, 363–374.

Moriishi, K., Matsuura, Y., 2007. Host factors involved in the replication of hepatitis C virus. Rev. Med. Virol. 17, 343–354.

Noack, J., Bernasconi, R., Molinari, M., 2014. How viruses hijack the ERAD tuning machinery. J. Virol. 88, 10272–10275.

Oostra, M., Hagemeijer, M.C., van Gent, M., Bekker, C.P., te Lintelo, E.G., Rottier, P.J., de Haan, C.A., 2008. Topology and membrane anchoring of the coronavirus replication complex: not all hydrophobic domains of nsp3 and nsp6 are membrane spanning. J. Virol. 82, 12392–12405.

Oostra, M., te Lintelo, E.G., Deijs, M., Verheije, M.H., Rottier, P.J., de Haan, C.A., 2007. Localization and membrane topology of coronavirus nonstructural protein 4: involvement of the early secretory pathway in replication. J. Virol. 81, 12323–12336.

Prentice, E., McAuliffe, J., Lu, X., Subbarao, K., Denison, M.R., 2004. Identification and characterization of severe acute respiratory syndrome coronavirus replicase proteins. J. Virol. 78, 9977–9986.

Ratia, K., Pegan, S., Takayama, J., Sleeman, K., Coughlin, M., Baliji, S., Chaudhuri, R., Fu, W., Prabhakar, B.S., Johnson, M.E., Baker, S.C., Ghosh, A.K., Mesecar, A.D., 2008. A noncovalent class of papain-like protease/deubiquitinase inhibitors blocks SARS virus replication. Proc. Natl. Acad. Sci. USA 105, 16119–16124.

Reggiori, F., Monastyrska, I., Verheije, M.H., Cali, T., Ulasli, M., Bianchi, S., Bernasconi, R., de Haan, C.A., Molinari, M., 2010. Coronaviruses Hijack the LC3-I-positive EDEMosomes, ER-derived vesicles exporting short-lived ERAD regulators, for replication. Cell Host Microbe 7, 500–508.

Rust, R.C., Landmann, L., Gosert, R., Tang, B.L., Hong, W., Hauri, H.P., Egger, D., Bienz, K., 2001. Cellular COPII proteins are involved in production of the vesicles that form the poliovirus replication complex. J. Virol. 75, 9808–9818.

Snijder, E.J., van der Meer, Y., Zevenhoven-Dobbe, J., Onderwater, J.J., van der Meulen, J., Koerten, H.K., Mommaas, A.M., 2006. Ultrastructure and origin of membrane vesicles associated with the severe acute respiratory syndrome coronavirus replication complex. J. Virol. 80, 5927–5940.

Sparks, J.S., Lu, X., Denison, M.R., 2007. Genetic analysis of Murine hepatitis virus nsp4 in virus replication. J. Virol. 81, 12554–12563.

Subissi, L., Posthuma, C.C., Collet, A., Zevenhoven-Dobbe, J.C., Gorbalenya, A.E., Decroly, E., Snijder, E.J., Canard, B., Imbert, I., 2014. One severe acute respiratory syndrome coronavirus protein complex integrates processive RNA polymerase and exonuclease activities. Proc. Natl. Acad. Sci. USA 111, E3900–E3909.

Tanaka, T., Kamitani, W., DeDiego, M.L., Enjuanes, L., Matsuura, Y., 2012. Severe acute respiratory syndrome coronavirus nsp1 facilitates efficient propagation in cells through a specific translational shutoff of host mRNA. J. Virol. 86, 11128–11137.

Thanigaimalai, P., Konno, S., Yamamoto, T., Koiwai, Y., Taguchi, A., Takayama, K., Yakushiji, F., Akaji, K., Chen, S.E., Naser-Tavakolian, A., Schon, A., Freire, E., Hayashi, Y., 2013. Development of potent dipeptide-type SARS-CoV 3CL protease inhibitors with novel P3 scaffolds: design, synthesis, biological evaluation, and docking studies. Eur. J. Med. Chem. 68, 372–384.

Thiel, V., Ivanov, K.A., Putics, A., Hertzig, T., Schelle, B., Bayer, S., Weissbrich, B., Snijder, E.J., Rabenau, H., Doerr, H.W., Gorbalenya, A.E., Ziebuhr, J., 2003. Mechanisms and enzymes involved in SARS coronavirus genome expression. J. Gen. Virol. 84, 2305–2315.

Tsang, K.W., Ho, P.L., Ooi, G.C., Yee, W.K., Wang, T., Chan-Yeung, M., Lam, W.K., Seto, W.H., Yam, L.Y., Cheung, T.M., Wong, P.C., Lam, B., Ip, M.S., Chan, J., Yuen, K.Y., Lai, K.N., 2003. A cluster of cases of severe acute respiratory syndrome in Hong Kong. N. Engl. J. Med. 348, 1977–1985.

Ulasli, M., Verheije, M.H., de Haan, C.A., Reggiori, F., 2010. Qualitative and quantitative ultrastructural analysis of the membrane rearrangements induced by coronavirus. Cell Microbiol. 12, 844–861.

Zaki, A.M., van Boheemen, S., Bestebroer, T.M., Osterhaus, A.D., Fouchier, R.A., 2012. Isolation of a novel coronavirus from a man with pneumonia in Saudi Arabia. N. Engl. J. Med. 367, 1814–1820.